Received: 8 June 2023 | Revised: 26 July 2023 | Accepted: 27 September 2023

DOI: 10.1002/jemt.24438

RESEARCH ARTICLE

MICROSCOPY RESEARCH & TECHNIQUE WILEY

Fabrication of wound dressings: Herbal extract-loaded nanoliposomes embedded in fungal chitosan/polycaprolactone electrospun nanofibers for tissue regeneration

Sevim Feyza Erdoğmuş [1] | Özlem Erdal Altintaş [2] | Hasan Hüseyin Demirel [3] | Nurullah Okumuş [4]

[1]Department of Basic Pharmaceutical Sciences, Faculty of Pharmacy, Afyonkarahisar Health Sciences University, Afyonkarahisar, Turkey

[2]Department of Medical Services and Techniques, Şuhut Vocational School of Health Services, Afyonkarahisar Health Sciences University, Afyonkarahisar, Turkey

[3]Afyon Kocatepe University, Bayat Vocational School, Department of Laboratory and Veterinary Health, Afyonkarahisar, Turkey

[4]Afyonkarahisar Health Sciences University, Faculty of Medicine, Department of Pediatrics, Afyonkarahisar, Turkey

Correspondence
Sevim Feyza Erdoğmuş, Department of Basic Pharmaceutical Sciences, Faculty of Pharmacy, Afyonkarahisar Health Sciences University, Afyonkarahisar 03030, Turkey.
feyzakus@gmail.com; feyza.erdogmus@afsu.edu.tr

Review Editor: Mingying Yang

Abstract

Wound healing is a complex process and one of the major therapeutic and economic subjects in the pharmaceutical area. In recent years, the fabrication of nano-sized wound dressing models has attracted great attention for tissue regeneration. Plant extracts loaded nanoparticles are environmentally friendly and non-toxic and the release of the bioactive substance will be controlled to the wound area. This study aims to fabricate wound dressing models that contain bioactive components for tissue regeneration. Fungal chitosan/polycaprolactone nanofiber was fabricated by electrospinning and it has been characterized. Plant extracts loaded nanoliposomes were prepared, characterized, and embedded in nanofiber structures. The effectiveness of wound dressing models for tissue regeneration was evaluated by in vitro and in vivo studies. It was observed that all wound dressing models positively affect the cell viability of human dermal fibroblast cells. It was determined that plant extracts loaded nanoparticles embedded in nanofibers increased in cell viability than nanoparticles that were non-embedded in nanofiber structures. Histological analysis showed that plant extract-loaded nanoliposomes embedded in chitosan/PCL nanofibers were used for tissue regeneration. The most effective nanofibers were determined as Wd-CINL nanofibers.

Research Highlights

- *Hypericum perforatum* L. and *Cistus laurifolius* L. were prepared by modified ultrasonic extraction method.
- Fungal chitosan/polycaprolactone nanofiber was fabricated by electrospinning and it has been characterized.
- Plant extract-loaded nanoliposomes were prepared, and characterized.
- They were embedded in chitosan/polycaprolactone nanofiber.
- Effects of the wound dressing model were analyzed by in vitro and in vivo assays for tissue regeneration.

KEYWORDS

Cistus lourifolius, *Hypericum perforatum*, nanofiber, nanoliposome

1 | INTRODUCTION

Wound healing is a complex process that consists of a sequence of molecular and cellular cases to tissue regeneration. It involves the spatial and temporal synchronization of a variety of cell types with distinct roles in the phases of inflammation, proliferation (neo-angiogenesis, granulation, re-epithelialization), and maturation (extracellular matrix [ECM] remodeling) (Broughton et al., 2006; Gonzalez et al., 2016; Rodrigues et al., 2019; Vargas et al., 2010). Wound healing is one of the major therapeutic and economic subjects in the pharmaceutical area (Schreml et al., 2010) Although new products related to wound healing are constantly being developed there is no concurrence on the properties of an ideal wound dressing for tissue regeneration (Dorai, 2012; Maver et al., 2015; Pereira & Bartolo, 2016). In recent years, the production of nano-sized wound dressing models from biopolymers by electrospinning method has great attention (Chen et al., 2017; Ravichandran et al., 2022; Subbiah et al., 2005).

Electrospinning is a simple, effective, versatile, and widely used technique that allows the production of nanosized fibers from different polymers depending on the properties of the polymer and processing conditions (Huang et al., 2003; Ramakrishna et al., 2005). In this study, fungal chitosan which is a natural, antimicrobial, biodegradable biopolymer, and polycaprolactone (PCL) which is biocompatible were used to electrospun nanofiber webs for wound dressing applications.

Medicinal and aromatic plants have been used in ancient times for food, cosmetic purposes, and medicinal properties. Many recent studies have focused on therapeutic agents that can be obtained from natural sources for the treatment of wounds due to their low risk of side effects (Agyare et al., 2014; Budovsky et al., 2015; Palamthodi & Lele, 2014). Among these plants are *Hypericum perforatum* L. and *Cistus laurifolius* L. which have medical importance and are conventionally used and were selected in this study for the increase in wound healing efficacy (Adams & Graves, 2013; Eroglu et al., 2019; Sadhu et al., 2006; Suntar et al., 2010). *Cistus* spp. are rich in bioactive components such as flavonoids, polyphenols, and terpenoids and these compounds are anti-inflammatory, antibacterial, antifungal, antiviral, analgesic, antitumoral, and wound healing (Barros et al., 2013; Benali et al., 2020; Ehrhardt et al., 2007; Küpeli et al., 2006; Sayah et al., 2017; Stepien et al., 2018). *H. perforatum* L. which is commonly used to accelerate the healing of tissue regeneration has been proven by studies to have a positive effect on wound healing. Also, one of the promising ways to promote bioactive components' efficacy is to bring them to the nanostructures, control their release in the form of sustained delivery systems to the wound site, and enhance permeability. Plant extracts and their bioactive compounds which are used in nanoformulations have demonstrated high activity in the treatment of wounds in previous studies (Hajialyani et al., 2018). Different types of nanosized lipid-based drug delivery systems showed better applicability and enhanced skin penetration in wound healing therapy compared with conventional treatments. Their applications show potential for overcoming impediments in wound healing (Matei et al., 2021).

In this study, electrospun fungal chitosan/PCL nanofiber structures (Wd) were fabricated and *H. perforatum* L. and *C. laurifolius* L. extracts loaded nanoliposomes and they were embedded in nanofiber webs to increase tissue regeneration. Although electrospinning of chitosan/PCL was previously studied, the fungal chitosan obtained from *R. oryzae* in our previous study was used for the first time for the fabrication of electrospun nanofibers in this study. Also, no study has been found on *H. perforatum* L. and *C. laurifolius* L. plant extracts loaded nanoliposomes embedded in nanofibers, and this study focused on the controlled delivery of wound healing agents to wound healing treatment. The effectiveness of wound dressing models for tissue regeneration was evaluated by in vitro and in vivo studies.

2 | MATERIALS AND METHODS

2.1 | Animal ethics statement

The present study was conducted in compliance with the Animal Welfare Act, the implementing Animal Welfare Regulations, and the principles of the Guide for the Care and Use of Laboratory Animals, National Research Council. The study protocol was approved by the Animal Ethics Committee of Afyon Kocatepe University (number 49533702/175).

2.2 | Extraction of plant material

H. perforatum L. and *C. laurifolius* L. were collected from the Sandıklı-Afyonkarahisar region (Turkey) in June 2021. Prof. Dr. Mustafa Kargioglu in Afyon Kocatepe University, Faculty of Science and Letters, Department of Molecular Biology and Genetics. The aerial part of *H. perforatum* L. and leaves of *C. laurifolius* L. were dried and they were turned into a fine powder by a mill. The modified ultrasonic extraction method was used to prepare plant extract. 30 g powdered each of *H. perforatum* L. (Hp) and *C. laurifolius* L. (Cl) were prepared with 400 mL MeOH and ultrasonicated for 1 h, at room temperature (Latiff et al., 2021). The available aqueous extract was filtered through Whatman filter paper No. 1. Solvents in the extracts were evaporated in a rotary evaporator (Heidolph) at 40°C and followed by freeze-drying.

2.3 | Fabrication of electrospun fungal chitosan/PCL-based nanofiber

The chitosan of *R. oryzae* obtained from our previous study (AFSU-BAP Project No. 19. TEMATİK. 005) was used for the fabrication of electrospun nanofibers (Erdoğmuş et al., 2023). In this procedure: 2% fungal chitosan /EDTA (2:1) and 12% PCL 3:7 were prepared in trifluoroethanol (TFE) solutions were stirred on a magnetic stirrer overnight to obtain a homogenous polymer solution) (Dhandayuthapani et al., 2010; Levengood et al., 2017). The electrospinning conditions: flow rate (mL/h): 0,30, voltage (kV): 20, spinnerette-collector distance (mm): 200, drum speed (rpm): 55, and oscillation range (mm): 20.

The morphology of the fungal chitosan/PCL nanofiber was analyzed by scanning electron microscopy (SEM). The samples were sputter-coated with gold for 30 s at 100 mA before imaging with an LEO 1430 VP SEM (Carl Zeiss AG, Jena, Germany) at an accelerating voltage of 20 kV. The diameter of the electrospun fibers was determined from SEM images.

2.4 | Preparation of nanoliposomes and characterization

Plant extracts loaded nanoliposomes were prepared according to Khoshraftar et al. (2020). In this assay: 30 mL of ethanol (96%) with 1 g of phosphatidylcholine was continuously stirred at 50°C for 1 h until the complete dissolution of lecithin was achieved. The solvent was then evaporated by a rotary evaporator (Heidolph, Germany). Each plant extract (1.5 g) was dissolved in 36 mL of phosphate buffer at ambient temperature and it was mixed with the sample (phosphatidylcholine layer). Then, the prepared nanoliposomes were sonicated in an ultrasonic bath for 2 min at 40°C and it was dried in the oven dryer at 60°C for 48 h. The characterizations of nanoliposomes were analyzed by SEM, dynamic light scattering method (DLS), and Zeta potential. The mean particle size and polydispersity index (PDI) were measured (Khoshraftar et al., 2019). To extract loaded nanoliposomes embedded in nanofiber webs, 1% plant extract loaded nanoliposomes were sprayed into fungal chitosan/PCL nanofiber webs and dried in ambient conditions, and washed with dH_2O. SEM analysis was performed to determine whether the nanoliposomes were embedded into the nanofibers.

2.5 | In vitro release test

Firstly, plant extracts were dissolved in PBS buffer at different concentrations, and the absorbances were measured with a UV spectrophotometer and a standard calibration curve was prepared. To examine the release profiles of plant extract loaded nanoliposomes embedded in nanofiber groups were cut into squares with 1 cm x 1 cm and placed into tubes that contained PBS buffer (pH:7.4) and incubated in a water bath at 37°C. Samples were taken from the medium at certain time intervals (0, 10, 20, 30, 40, 60, 80, 100, 120, 140, 160, 180, 200, 220, and 240 min) and absorbance was measured by UV- spectrophotometer (Cesur, 2022).

2.6 | Swelling test

The dry weight of the nanofibers (W_d) was measured for the determination of swelling (%). The nanofibers were placed in tubes that contained phosphate-buffered saline (PBS, pH 7.4) and kept in a water bath at 37°C. At certain time intervals (0, 10, 20, 30, 40, 60, 80, 100, 120, 140, 180, and 220 min), the nanofiber samples were removed from the PBS, and the excess water was removed with the help of filter paper and weighed again (W_w). Determination of the percent swelling of nanofiber was calculated according to Equation (1) equation (Ahamed & Sastry, 2011).

$$\%Swelling = [(W_w - W_d)/W_d] \times 100, \quad (1)$$

2.7 | In vitro biocompatibility test of wound dressing models

The biocompatibility of the fungal chitosan/PCL nanofiber and plant extract-loaded nanoliposomes embedded in nanofiber groups were assessed by MTT 3-[4,5-dimethylthiazol-2-yl]-2,5-diphenyl-tetrazolium bromide) cell proliferation on human dermal fibroblast cell line (HDFa, ATCC, PCS-201-012). Firstly, all nanofibers were cut into squares with 1 cm x 1 cm, placed into 24-well cell culture plates, and sterilized by UV light at 2 h. For stabilization, samples were left in the cell culture medium at 37°C overnight before cell seeding. HDFa cell lines were seeded onto the nanofibers at a density of 2×10^4 cells/well for each sample. The culture plates were incubated for 24 and 48 h in a CO_2 incubator (5%) at 37°C. After the incubation period, MTT reagent (10% v/v) was added directly onto the nanofibers containing well plates and incubated for 3 h. The formed formazan crystals were dissolved in (0.5% v/v) DMSO. The absorbance was measured at 570 nm by Gen5 Biotech® Microplate Reader. The medium was used as negative control and considered 100% viable. All experiments were performed in triplicate and under aseptic conditions. The biocompatibility of the nanofiber matrices was expressed as cell % viability, which was calculated from the ratio between the number of cells treated with the nanofibers. Twenty measurements assayed each nanofiber variant (Demirci et al., 2020).

2.8 | Design of animal experiments

For the in vivo experiments, male Wistar albino rats weighing 250–300 g were used. They were randomly separated into six groups of nine in each group. The design of the animal groups is shown in Table 1. The

TABLE 1 Design of experimental animal groups.

Group codes	Burned treatment
NC	Untreated
PC	Treated by Tegaderm
WD	Treated by chitosan/PCL nanofiber
WD-ClNL	Treated by *C. laurifolius* L. extract-loaded nanoliposomes embedded in chitosan/PCL nanofiber
WD-HpNL	Treated by *H. perforatum* L. extract-loaded nanoliposomes embedded in chitosan/PCL nanofiber
WD-ClHpNL	Treated by *C. laurifolius* L. and *H. perforatum* L. extract-loaded nanoliposomes embedded in chitosan/PCL nanofiber

untreated group was used as the negative control and commercially available wound dressing (Tegaderm) was used as the positive control.

2.9 | Creation of burn wounds

Rats were anesthetized with 40 mg/kg of ketamine ve 87 mg/kg of xylazine. The second-degree burn wound model was performed by exposing the shaved buckskin of anesthetized animals to hot water. For this procedure, a 1 cm diameter metal plaque was kept in hot water at 94 ± 1°C for 60 s then applied on the backs of rats and held for 15 s to burn the wound model (Khodja et al., 2013; Uhl et al., 2001). After the formation of standard, second-degree burn wounds, each nanofiber was applied to the burned areas. They were housed in a sterilized cage with a 12 h light/dark cycle and at a constant temperature (25 ± °C) and humidity (60 ± 5%). During the change of the wound dressing (Table 1) on the 1st, 3rd, 7th, 14th, 21st, and 24th days, the wound areas were imaged to calculate the wound width by the Image J program. Equation (2) was used to calculate the rate of wound closure (Walker & Mason, 1968).

$$\text{Wound area}\% = \left[\left(\text{Wound area}_{\text{on day}}\right)/\text{Wound area}_{\text{measured on day 1}}\right] \times 100, \quad (2)$$

Wound healing percentage = 100 − the percentage of the wound area.

2.10 | Histopathological study

Tissue samples were taken from each treatment model for histological observation on the 1st, 3rd, 7th, 14th, 21st, and 24th days by full-thickness skin biopsies, and the degree of healing was evaluated. All biopsy specimens were 3-mm punched. Biopsies are divided into two halves for ultrastructural studies. In all cases, the dissection was carried out at the end of the healing phase. The skin tissues were fixed with 10% formalin. After fixation, samples were embedded in paraffin, cut into 5 μm frozen sections with a cryostat microtome (Leica RM2245; Leica, Heidelberg, Germany), and then stained with hematoxylin–eosin reagent (Pachuau, 2015). The histopathologic examination was performed under a microscope (Nikon Ci-S microscope, Nikon DS-Fi3 camera, NIS-Elements D image analysis). Inflammation, re-epithelialization, neovascularization, ulcus, scar, and collagen accumulation were evaluated. No finding (−) was scored as 0, partial/poor (+) was scored as 1, completed but immature or mild (++) was scored as 2, completed and mature/moderate (+++) was scored as 3, and significant (++++) was scored as 4.

2.11 | Statistical analysis

Statistical analysis was carried out using the SPSS 22 statistical software program. The one-way ANOVA test was used to evaluate the research findings. The Duncan test was used to compare statistically different outcomes. The statistical significance level of <0.05 was accepted.

3 | RESULTS

3.1 | Fabrication of electrospun chitosan/PCL-based nanofiber

The image of the electrospun fungal chitosan/PCL nanofibers by the SEM analysis is given in Figure 1. It was determined that the nanofiber structure was uniform morphological structure, resistant to shrinkage, flexible, and can be easily removed from the surface on which it is formed, without breaking down.

3.2 | Preparation of nanoliposomes and characterization

The nanoliposomes that loaded *H. perforatum* L. extract (HpNL), and *C. laurifolius* L. extract (ClNL) were obtained and they were characterized by SEM, dynamic light scattering method (DLS), and zeta potential. The images of nanoliposomes are shown in Figure 2.

Particle size and distribution are some of the most important characteristics of nanoparticular systems. This feature determines the targetability, toxicity, stability of nanoparticles, drug loading capacity, and drug release of nanoparticular systems. The zeta potential is important in assessing the stability of colloidal distributions. The higher the zeta potential, the better the stability of the colloidal distributions. Colloidal particles adsorb ions in the dispersion medium. They are positively and negatively charged. Depending on whether each particle is positively or negatively charged, it can be surrounded by ions in the opposite direction. The results of the DLS analysis of nanoliposome structures are shown in Figure 3. ClNL

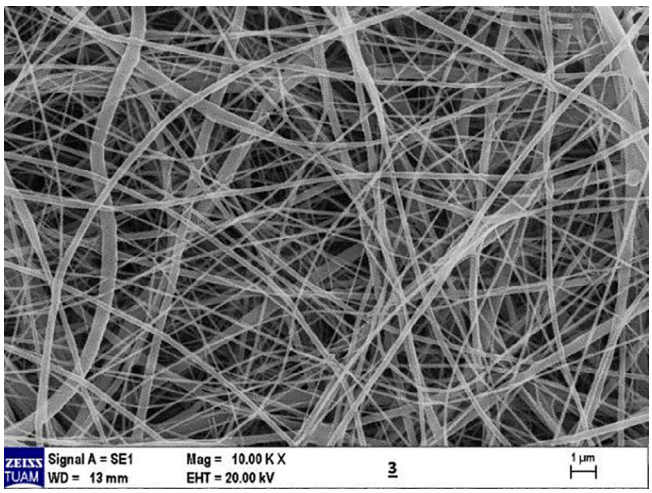

FIGURE 1 The image of the electrospun fungal chitosan/PCL nanofibers by SEM analysis.

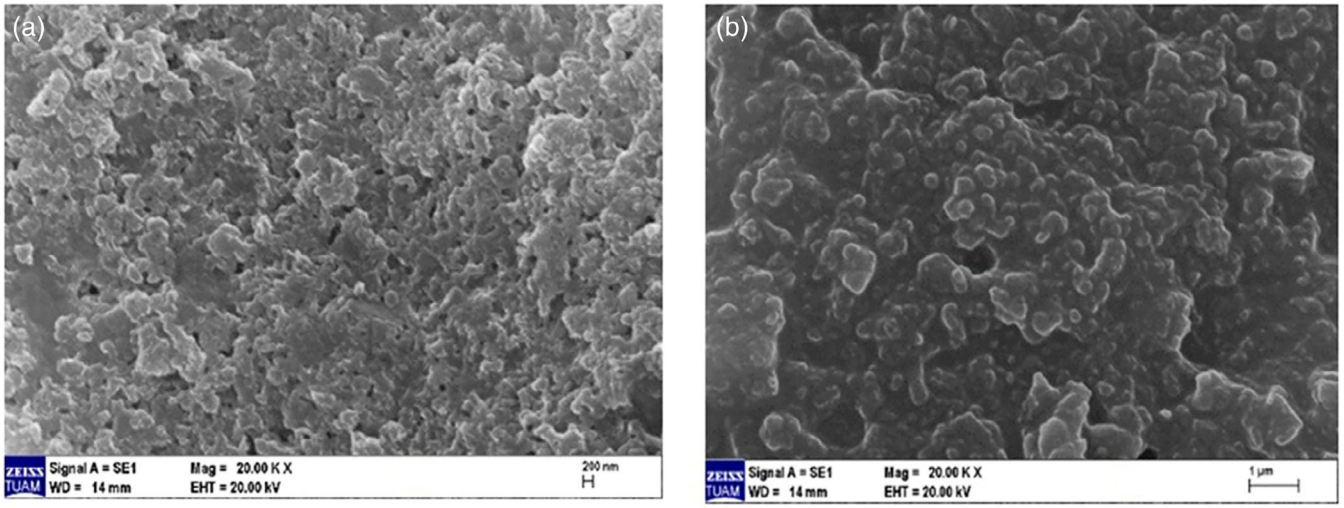

FIGURE 2 The images of ClNL and HpNL by SEM analyses.

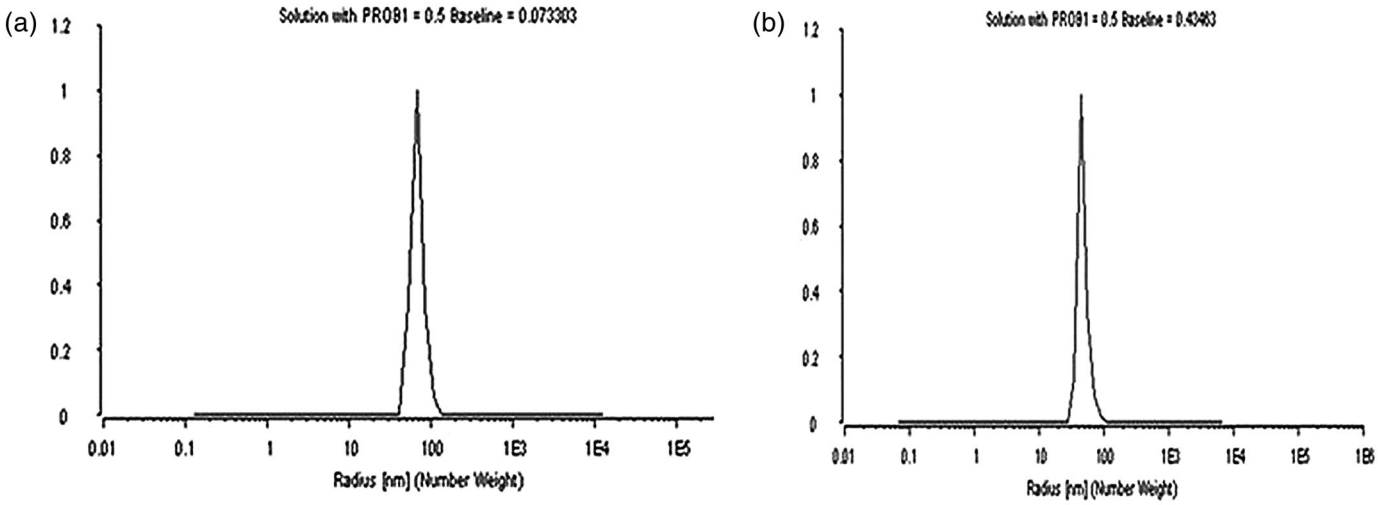

FIGURE 3 The results of DLS analysis for ClNL (a) (PDI = 0.51) and HpNL (b) (PDI = 0.59).

and HpNL structures' average sizes were determined as 80 nm and 63.7 nm, respectively. The polydispersity index (PDI), which means heterogeneity distribution, was determined. The zeta potential of ClNL and HpNL were determined as −27.9 and − 20 mV and are shown in Figures 4 and 5.

3.3 | Arrangement of herbal extracts loaded nanoliposomes embedded in nanofibers

After ClNL and HpNL were characterized they were embedded in the electrospun fungal chitosan/PCL nanofiber webs to increase tissue regeneration. When the results of the SEM analysis (Figure 6) were examined, it was seen that plant extract-loaded nanoliposomes were embedded in nanofiber structures.

3.4 | In vitro release and swelling test

Determination of in vitro release profiles of ClNL, HpNL, and HpClNL embedded nanofibers calibration curves of plant extract were determined (Figures S1 and S2). In vitro release profiles of ClNL, HpNL, and HpClNL embedded nanofibers are shown in Figure 7. According to the results of in vitro release profiles, the rapid plant extract release was determined within the first 30 minutes, and then a slower and more controlled release rate was observed. The release profile of nanofibers showed close values within the first 20 minutes and differences were observed in these values over time. It was determined that the extract released from the HpNL-embedded nanofiber released higher extracts than other nanofibers.

The results of the swelling ratios of nanofibers are shown in Figure 8. It has been observed that plant extract-loaded

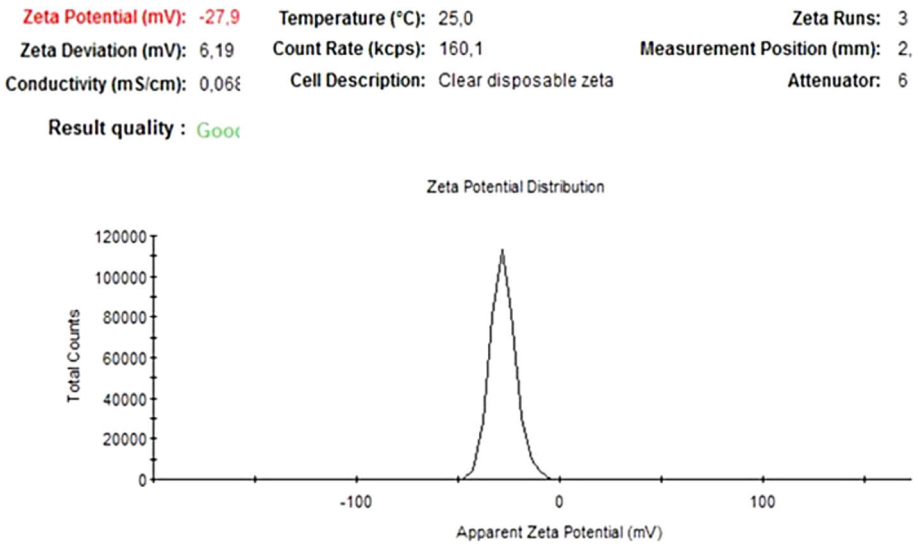

FIGURE 4 The zeta potential results of ClNL.

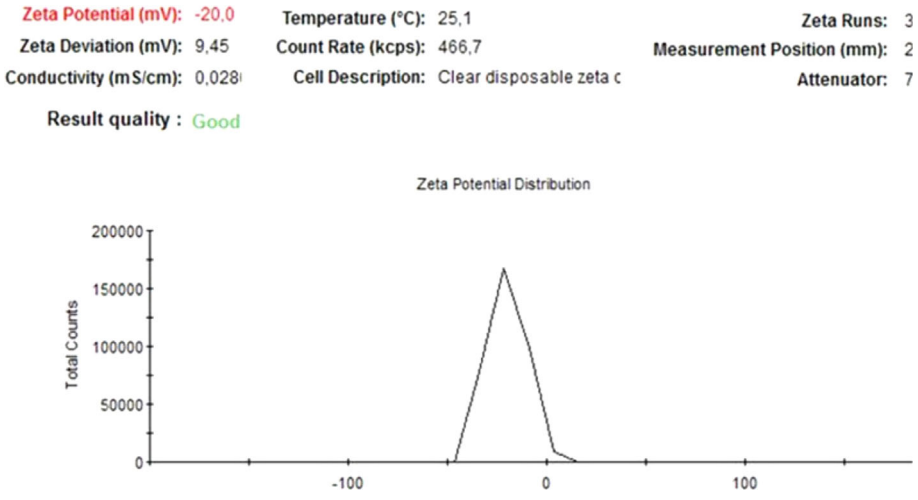

FIGURE 5 The zeta potential results of HpNL.

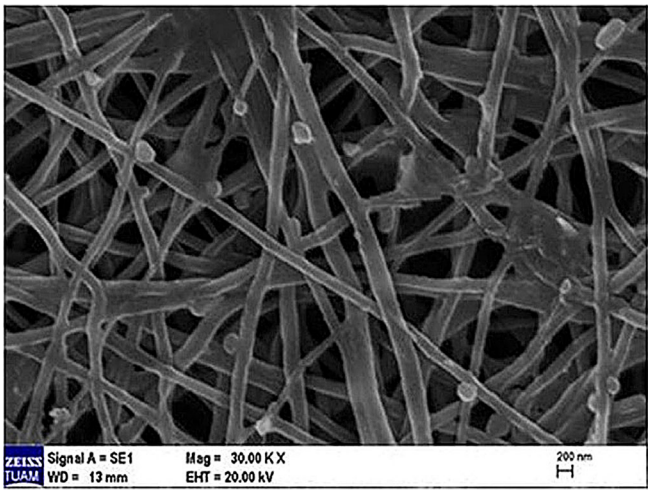

FIGURE 6 The image of plant extract-loaded nanoliposomes embedded in the nanofiber structure.

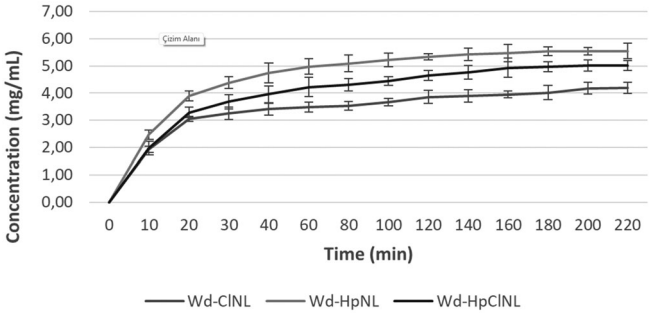

FIGURE 7 In vitro release profiles of ClNL, HpNL, and HpClNL embedded nanofibers.

nanoliposomes embedded in the nanofibers cause an increase in the water-holding capacity of the nanofibers. A rapid increase in the swelling of nanofibers was observed in the first hour and it was

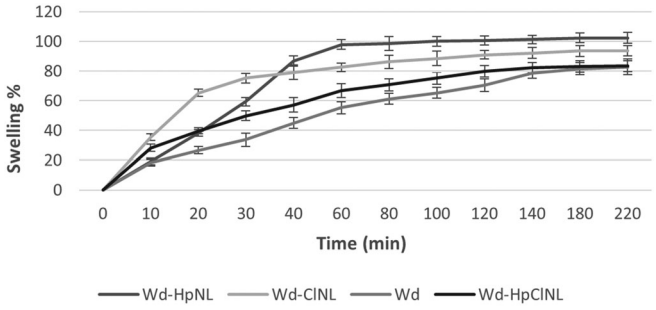

FIGURE 8 The results of the swelling ratios of nanofibers.

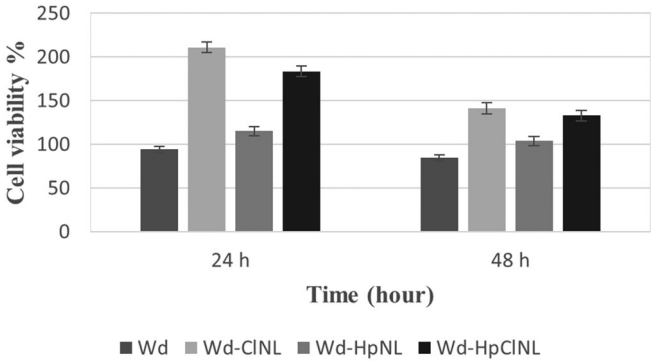

FIGURE 9 The results of in vitro biocompatibility of wound dressing models.

determined that this rapid increase decreased as time progressed and remained constant thereafter.

3.5 | In vitro biocompatibility test of wound dressing models

To determine the effectiveness of developed wound dressing models was evaluated by in vitro and in vivo studies. The biocompatibility of the chitosan/PCL nanofiber (Wd) and plant extract-loaded nanoliposomes embedded in nanofiber groups were assessed and the results are shown in Figure 9. As a result of the study, it was determined that the most effective nanofiber on the % viability of HDFa cells was ClNL loaded nanofibers. Then, ClNL and HpNL loaded nanofibers and Hp-NL loaded nanofibers were effective on HDFa cells. The lowest effect on viability% was observed in the unloaded nanofiber group.

3.6 | Effectiveness of wound dressing models

The wound healing % of wound dressing groups compared to PC and NC groups are shown in Figure 10. The wound dressing models that plant extract loaded nanoliposomes were more effective than the Wd group in wound healing and they were found to be as effective as the PC group. The most effective group for wound healing was determined as Wd-HpNL within 7 days. Wd-HpNL and Wd-HpClNL groups showed similarity to wound healing within 14–24 days.

The effects of treatment groups on reepithelialization, scar, neovascularization, inflammatory cell, and collagen effect in the second-degree burn model are shown in Figure 11. In the histopathological examination for inflammation, the preparations were evaluated according to the inflammatory cell density. The inflammations were observed in the wounds of the treatment and control groups for application days. It was observed that 90% of wounds of the Wd-ClNL and Wd-HpClNL, 80% Wd, Wd-HpNL, and 60% PC, 50% NC groups on the 3rd day. It was determined that 30% inflammation in wounds of the NC group and the other groups this value was determined 80% on the 7-14th day. The inflammation values of wounds of the Wd-ClNL, Wd-HpNL Wd-HpClNL groups were determined as 90% high, and 10% moderate levels. The inflammation was determined as 80% high, 10% moderate, and 10% low levels in the Wd group and 50% high, 30% moderate, and 20% low levels in the PC and NC groups on the 21st day.

The collagen formation was determined as 80% high, 10% moderate, and 10% low levels in the wounds of the Wd-HpNL, Wd-ClNL and 90% high, 10% low levels in the wounds of Wd-HpNL and 50% high, 50% low levels in the Wd group. These rates were found to be 100% low level in the NC and PC groups on 3rd day. It was observed that 80% high, 10% moderate levels in the Wd-ClNL, 50% high, and 50% low levels in the Wd-HpClNL and Wd-HpNL, Wd, NC and 90% high, 10% moderate collagen formation levels in the PC on 7th day. It was determined that collagen formations were found to be 80% high, 10% moderate levels in the Wd-ClNL, Wd-HpClNL and 50% high, 40% low levels in the Wd, Wd-HpNL and 80% high, 20% moderate levels in the PC, 50% high, 50% low levels in the NC on 14th day. Also, we observed that the collagen formations had 80% high, 10% moderate, and 10% low levels in the Wd-ClNL, Wd-HpClNL and 80% high, 20% moderate levels in the Wd-HpNL and 90% moderate, 10% low levels in the Wd, PC and 80% high, 10% moderate, 10% low levels in the NC group on 21st day.

When the neovascularization levels of in vivo groups were compared on the 3rd day, 80% high, 10% moderate, and 10% low levels of vascular proliferation were observed in wounds of Wd-HpClNL, Wd-ClNL groups, and these rates were found to be 50% high, 30% moderate, 10% low levels of wounds in Wd-HpNL group. It was observed that these rates were low at 10% moderate, and 50% low levels of wounds the in the Wd, PC groups. Vascular proliferation was detected in 20% of low levels of wounds in the NC group. These rates were observed at 80% high, and 20% low levels of wounds in the Wd-Hp-ClNL, Wd-ClNL while it is in the Wd-Hp, Wd groups, these rates were found to be 90% high and 10% moderate levels. Also, these rates were found as 50% high, 30% moderate, and 20% low vascular proliferation in the NK and PK groups on the 7th day. It was observed that 90% high and 20% moderate levels of vascular proliferation formation in Wd-HpClNL, and Wd-

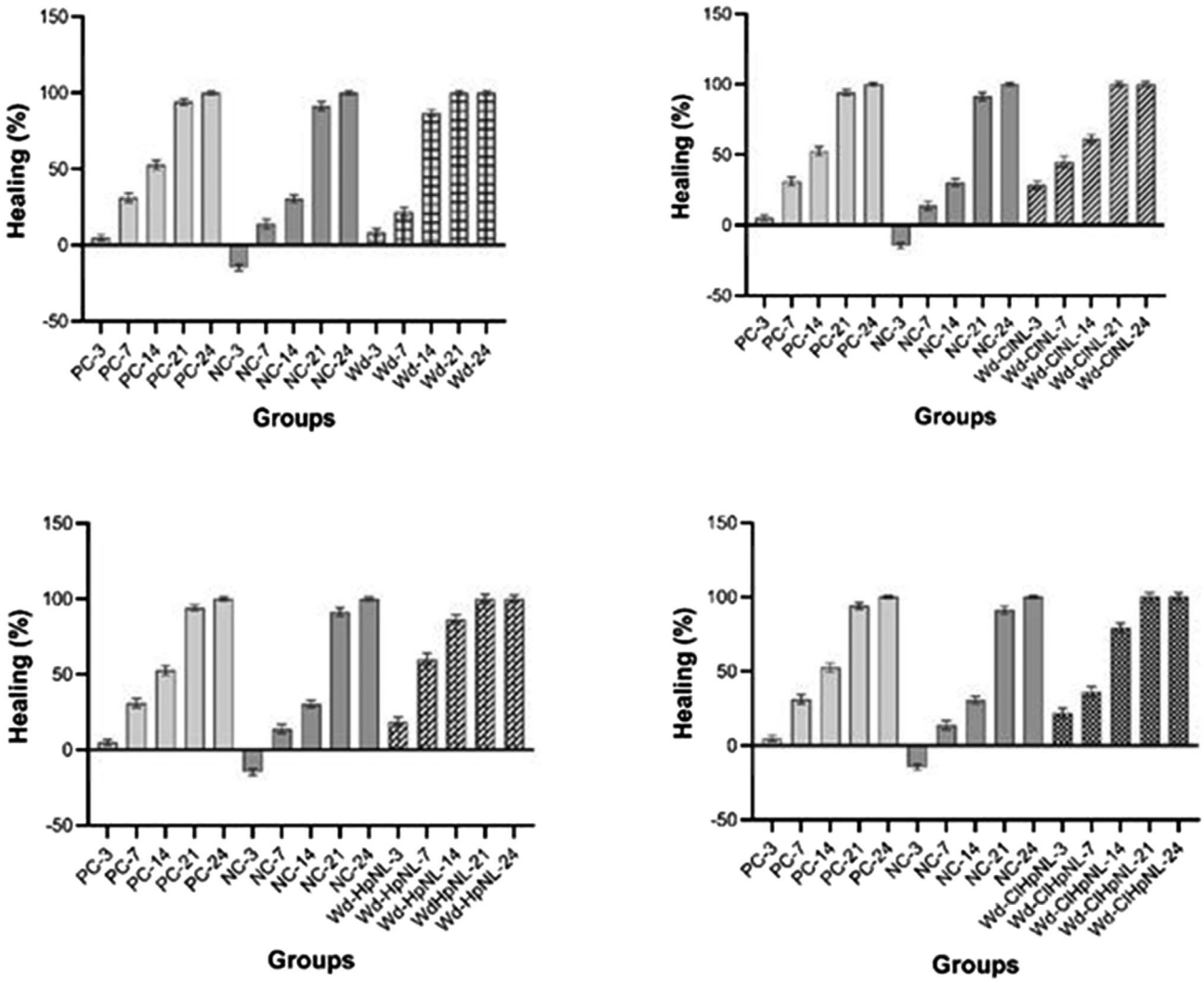

FIGURE 10 Wound healing % of wound dressing models to compare with PC and NC groups.

ClNL groups. 80% high and 20% moderate vascular proliferation was observed in the Wd-HpNL and Wd groups, While these rates were seen as 80% high, 10% moderate levels in the NC and PC groups on the 14th day. When the 21st-day preparations were examined, these rates were 90% high, 10% moderate in the Wd-HpClNL, and Wd-ClNL, and 80% high, 20% moderate levels in the Wd-HpNL groups. Also, these rates were found to be 80% high, and 20% moderate levels in the NC and PC groups.

When the reepithelialization levels were compared, 80% high, 10% moderate, and 10% low levels in the Wd-HpClNL, and Wd-ClNL. It was observed that these rates were found as 80% high, 20% moderate in the Wd-HpNL group, 80% high, 10% low levels in the Wd group, and 40% high, 10% low levels in the PC, NC groups on the 7th day. The reepithelialization rates were observed at 80% high, 10% moderate, and 10% low in the Wd-HpClNL, and Wd-ClNL groups and 90% high and 10% mild levels in the Wd-HpNL group. These rates were found as 80% moderate, 20% low levels in the Wd, and PC groups, and 20% high, and 50% low levels in the NC on the 14th day. When the 21st-day preparations were examined, these rates were 90% high, 10% moderate levels in the Wd-HpClNL, Wd-ClNL, and Wd-HpNL groups and 50% high, 30% moderate, 20% low levels in the Wd, PC groups.

When the scar and ulcus formation rates were compared on the 3rd-day preparations, 20% moderate, 80% low levels in the Wd-HpClNL, and Wd-ClNL groups, and low scar and ulcus formation was observed in the entire Wd-HpNL group and 50% moderate, 50% low levels in the Wd group and 90% moderate, 10% low levels in the NC, PC groups. These rates were found as 80% low, 20% moderate levels in the Wd-HpClNL, and Wd-ClNL groups, and 90% low levels in the Wd-HpClNL group on the 7th day. While these rates were 50% moderate, and 50% low levels in the Wd, and PC groups and 80% moderate and 20% low levels in the NC groups. When the 14th and 21st-day preparations were examined, scar and ulcus were not found in the Wd-HpClNL, Wd-ClNL groups. It was encountered at 10% on the 21st day in the Wd-HpClNL, and Wd groups. It was observed 10% moderate levels in the PC and NC groups. A comparison of the mean histological scores of the wounds in the treatment and control groups is shown in Table S1.

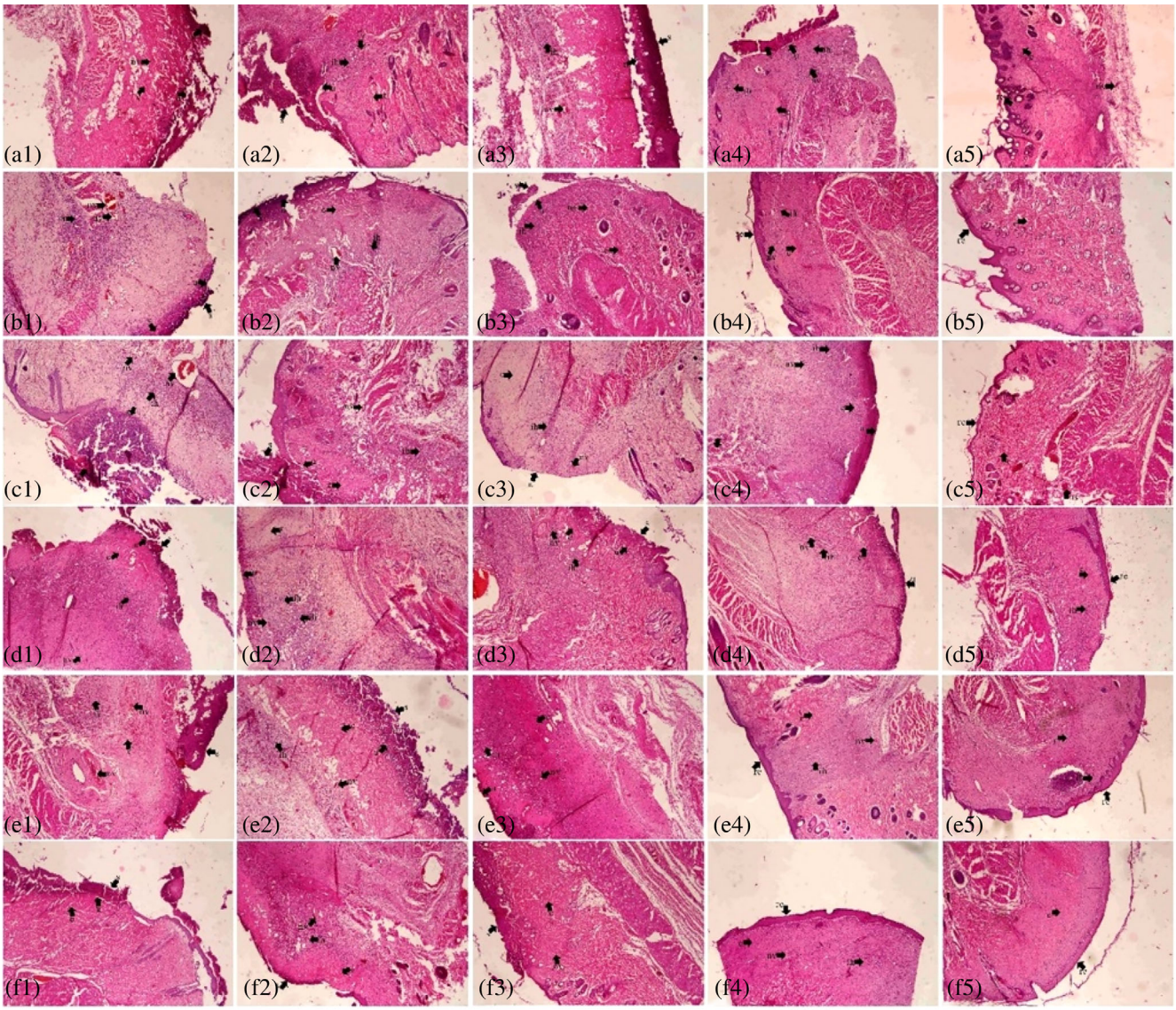

FIGURE 11 The histological features of in vivo treatment groups.

4 | DISCUSSION

Wound healing is a complex process and it involves the well-organized and highly complex interaction of different tissues and cells. An ideal wound dressing should be biocompatible, protect against bacterial infection, and provide adequate humidity. Controlled and localized delivery of wound-healing drugs to the wounds is more convenient than systemic administration (Sitterberg et al., 2010). The transportation of drugs or bioactive substances to the target area is one of the main problems in pharmaceutical and biotechnological fields. For this reason, drug delivery systems are used to transport drugs or active substances to the targeted area.

Previous studies revealed that the wound healing activity of plant extract and extract-loaded wound dressings and the promotion of wound healing through anti-inflammatory and antibacterial effects and the stimulation of angiogenesis and fibroblast activity has been demonstrated (Fathi et al., 2020). The results of this study revealed that the fungal chitosan/PCL wound dressing models have the same advantage as easily taking the shape of the area where it is applied to the wound dressing and having a high water holding capacity and

flexibility. The PCL is a durable material that gives it the ability to protect its form against external effects on the wound dressing. Since the nanofiber wound dressing designed in this study is considered a wound contact layer, it was desired to have a high water-holding capacity. The high swelling ratio of the developed wound dressing model has the desired properties for wound dressings. Chitosan is a biodegradable, biocompatible polymer that is used in wound dressing models in this study (Conti et al., 2000). It has been reported that chitosan accelerates tissue regeneration. Also, chitosan exhibits many advantages for topical application, non-irritancy, and antibacterial effects. Alemdaroğlu et al. (2006) showed that treatment with EGF-chitosan gel formulation decreased the wound healing period, accelerated epidermal regeneration, and stimulated granulation; tissue formation could be obtained. In another study, by Khodja et al. (2013), hydrogel-based PVA/chitosan was evaluated for tissue regeneration in a burn rat model. It has been reported that this hydrogel permits the regeneration of tissue elements in skin wounds and stimulates activity and/or can stimulate fibroblastic proliferation which releases interleukin-V and production of type III collagen, stimulatingstimulatingthe macrophage migration.

To increase the efficiency of the obtained nanofibers in tissue regeneration, plant extract-loaded nanoliposomes were added. *H. perforatum* L., and *C. laurifolius* L. which are among the medicinal plants and have anti-inflammatory, antimicrobial, analgesic, antitumoral, and wound-healing effects were used in this study. The extracts of *H. perforatum* and *C. laurifolius*-loaded nanoliposomes were successfully obtained and characterized by SEM and DLS. It was determined that the ClNL and HpNL average sizes are 80 nm and 63.7 nm, respectively. Zeta potential value is a very important parameter to have information about the long-term strength of nanomaterials. It plays an important role in determining the capacity of particles, especially for drug delivery applications by electrostatic interaction. The zeta potential of nanoparticles is ±30 mV, indicating that they are stable with surface loading, which prevents aggregation of particles in suspension. In general, forming aggregates is more difficult in high zeta potential systems. Formulations in the range of −31 to −60 mV, −61 to −80 mV, and − 81 to −100 mV are described as moderate, good, and excellent electrostatic stability, respectively (Müller & Keck, 2004). The zeta potential of ClNL was determined as −27.9 mV, and the HpNL was determined as −20 mV. The polydispersity index (PDI), which means the heterogeneity distribution, was determined. In another study by Poudel et al. (2009), it was reported that the zeta potential of the liposomes they obtained ranged from −9.8 to −14 mV Looking at the particle size distribution, it was observed that it ranged from 186 to 260 nm.

The integration of nanoliposomes into nanofibers was confirmed by SEM analysis. The release of plant extract from wound dressing models was determined by in vitro studies. The fastest substance release was observed in Wd-HpNL, followed this Wd-HpClNL, and the slowest release was observed in Wd-ClNL. Plant extract attached to the surface of nanofibers or attached to the surface with weak bonds have a higher diffusion rate and these molecules are released rapidly in the initial period. In the slower (controlled) substance release period, it takes a longer time for non-surface plant extract molecules to reach the surface (because it requires the degradation of some polymer units). According to the results of the swelling test, it has been observed that plant extract-loaded nanoliposomes embedded in the nanofibers cause an increase in the water-holding capacity of the wound dressing models.

In the last step of the study, the effectiveness of extract-release medical matrices in tissue regeneration was evaluated by in vitro and in vivo studies. The in vitro efficacy of nanofibers was tested on HDFa cells. As a result of the study, it was seen that nanofibers had a positive effect on the cell viability of HDFa cells. It was determined that there was an increase in cell viability in the nanofibers loaded with herbal nanoliposomes. It was determined that the most effective nanofibers were Wd-HpClNL nanofibers. Then, Wd-HPNL and Wd-HPClNL nanofibers were effective on cell viability, respectively. The lowest effect on cell viability was observed in the uncharged nanofiber group (Wd). Wistar albino male rats weighing 250–300 g were used to determine the in vivo efficacy of the developed wound dressing models. According to the results of in vivo studies, it was determined that nanoparticle-loaded medical matrices are more effective than positive control in the healing of second-degree burn wounds and have the potential to be used for treatment purposes. It has been determined that Wd-HPClNL nanofibers have higher healing efficiency than other nanofiber structures.

Statistically significant differences were determined between the application groups and the application durations when the results were evaluated histopathologically. The inflammation rates of wound dressing models were determined as higher than the PC and NC groups. The collagen formation rates of Wd-HPClNL, Wd-ClNL, and Wd-HPNL were higher than Wd, and NC groups and showed similarity with the PC group. When the neovascularization rates were compared with in vivo groups it was observed that high neovascularization rates in the Wd-HPClNL, Wd-ClNL, and followed Wd-HPNL. The highest epithelialization was observed in the Wd-HPClNL, Wd-ClNL groups and followed by Wd-HPNL, Wd groups. It was determined that the wound dressing models increased epithelialization compared to the positive control. When the scar and ulcus formation rates were compared the lowest rates were found in the Wd-HPClNL, Wd-ClNL groups and followed by Wd-HPNL, Wd groups. The epithelialization levels of wound dressing models were found to be higher than the PC and NC groups.

Similar to the present study Hashemi et al. (2022) investigated the electrospun polycaprolactone/chitosan/internal layer of oak fruit for potential application. The results of this study revealed that this wound dressing could be a promising candidate for biomedical application. In another study, Tord et al. (2020) assessed the histological, biochemical, and immunohistochemical evaluation of collagen/doxycycline-loaded nanofiber wound dressing. It was revealed that an effective and safe wound dressing has been developed to be used in wound healing. Fathi et al. (2020) investigated the effectiveness of electrospun chitosan, PVA, and silk nanofiber on the wound healing process by in vitro and in vivo assay. They reported that this structure is suitable for stem cell culture and application in tissue engineering

because of its biophysical properties and cytocompatibility. In another study, Levengood et al. (2017) developed electrospun chitosan/PCL nanofiber and they were evaluated as skin tissue engineering scaffolds using a mouse cutaneous excisional skin defect model. This study revealed that the nanofiber structures increased the wound healing rate, re-epithelialization, maturity of neo-epidermis, and collagen deposition when compared with the control (Tegaderm). The results of this study are similar to the results of our study on re-epithelization and collagen formation. Our results of the present study support the literature. Administration of anti-inflammatory and antioxidant agents may be beneficial in healing skin wounds. It has been reported that *H. perforatum* L. and *C. laurifolius* L. have higher potential antimicrobial, antioxidant, and anti-inflammatory activities. The efficacy of nanofibers that embedded nanoliposomes on wound healing may be related to their bioactive properties, which reduce the bacterial load of the wound and increase epithelial proliferation. It has been also reported in the literature that the analgesic and anti-inflammatory activities of *H. perforatum* L., *C. laurifolius* L. extracts accelerate capillary circulation and that the anti-inflammatory and antioxidant activities reduce the harm caused by free radicals formed as a result of the inflammation and prevent the progression of necrosis (Hajialyani et al., 2018). It has been reported that the hypoxic environment under moist wound dressings increased capillary proliferation; angiogenesis is faster in moist conditions (Boateng & Catanzano, 2015).

The most obvious results to unearth from this study are the wound healing rate of the plant extract-loaded nanoliposomes embedded in nanofiber, especially Wd-HPClNL and Wd-ClNL groups were significantly faster than the NC group, and that the healing rates in these groups were close to the PC group.

5 | CONCLUSION

The results of this study indicated that wound dressing models which combine the important intrinsic biological properties of chitosan and the mechanical integrity and stability of PCL were used as wound dressings for tissue regeneration. The fungal chitosan/PCL nanofiber structures have significant potential in promoting tissue regeneration and physical properties of nanofibers such as fiber diameter, swelling rate, and surface area as well as scaffold porosity and stiffness. The histological results indicated that wound dressing models supported wound healing more than the NC group and wound dressings in which plant extract-loaded nanoliposomes were embedded were as effective as the PC group in the second-degree burn wound healing process. Among these wound dressing models, the Wd-HpClNL group was better and more rapid when compared with the other groups. In this respect, since the preparation of *H. perforatum* L. and *C. laurifolius* L. extracts loaded nanoliposomes are easy and the economic aspects are favorable it could be used as an alternative treatment option in wound healing. The structure of nanoliposome-embedded nanofibers could increase their bioavailability, control release in the delivery systems to the wound site, and enhance the permeability of these therapeutics. The results of this study indicated that the wound dressing models that consist of plant extract-loaded nanoliposomes have the potential to be used in the treatment of second-degree burns.

AUTHOR CONTRIBUTIONS

Sevim Feyza ErdoĞmuŞ: Conceptualization; investigation; writing – original draft; methodology; validation; visualization; writing – review and editing; formal analysis; data curation; supervision; resources. **Özlem Erdal AltintaŞ:** Investigation; methodology; writing – review and editing; visualization; formal analysis. **Hasan Hüseyin Demİrel:** Methodology; visualization; data curation; formal analysis. **Nurullah OkumuŞ:** Writing – review and editing; writing – original draft; investigation.

ACKNOWLEDGMENTS

This study was supported by AFSU-BAP (Project No. 19. TEMATİK. 005).

CONFLICT OF INTEREST STATEMENT

The authors declare that they have no conflict of interest.

DATA AVAILABILITY STATEMENT

The raw/processed data required to reproduce these findings are available from the corresponding author on reasonable request.

ORCID

Sevim Feyza Erdoğmuş https://orcid.org/0000-0002-4319-7558
Özlem Erdal Altintaş https://orcid.org/0000-0003-4680-1738
Hasan Hüseyin Demirel https://orcid.org/0000-0002-4795-2266
Nurullah Okumuş https://orcid.org/0000-0001-6082-0818

REFERENCES

Adams, S., & Graves, N. (2013). Economic evaluation of St. John's wort (*Hypericum perforatum*) for the treatment of mild to moderate depression. *Journal of Affective Disorders*, *148*, 228–234. https://doi.org/10.1016/j.jad.2012.11.064

Agyare, C., Amuah, E., Adarkwa-Yiadom, M., Osei-Asante, S., & Ossei, P. P. K. (2014). Medicinal plants used for the treatment of wounds and skin infections: Assessment of wound healing and antimicrobial properties of *Mallotus oppositifolius* and *Momordica charantia*. *International Journal of Phytoremediation*, *6*, 50–58.

Ahamed, M. I. N., & Sastry, T. P. (2011). Wound dressing application of chitosan based bioactive compounds. *International Journal of Life Science*, *2*(8), 991–996.

Alemdaroğlu, C., Değim, Z., Celebi, N., Zor, F., Oztürk, S., & Erdoğan, D. (2006). An investigation on burn wound healing in rats with chitosan gel formulation containing epidermal growth factor. *Burns*, *32*(3), 319–327. https://doi.org/10.1016/j.burns.2005.10.015

Barros, L., Duenas, M., Aloes, C. T., Silvac, S., Henriques, M., Santos-Buelga, C., & Ferreiraa, C. F. R. I. (2013). Antifungal activity and detailed chemical characterization of *Cistus ladanifer* phenolic extracts. *Industrial Crops and Products*, *41*, 41–45. https://doi.org/10.1016/j.indcrop.2012.03.038

Benali, T., Bouyahya, A., Habbadi, K., Zengin, G., Khabbach, A., Achbani, H., & Hammani, K. (2020). Chemical composition and antibacterial activity of the essential oil and extracts of *Cistus ladaniferus* subsp. *ladanifer* and *Mentha suaveolens* against phytopathogenic bacteria and their ecofriendly management of phytopathogenic bacteria. *Biocatalysis and Agricultural Biotechnology*, *28*, 101696. https://doi.org/10.1016/j.bcab.2020.101696

Boateng, J., & Catanzano, O. (2015). Advanced therapeutic dressings for effective wound healing-a review. *Journal of Pharmaceutical Sciences*, *104*, 3653–3680.

Broughton, G., Janis, J. E., & Christopher, E. A. (2006). Wound healing: An overview. *Plastic and Reconstructive Surgery*, *117*, 1eS-32eS. https://doi.org/10.1097/01.prs.0000222562.60260.f9

Budovsky, A., Yarmolinsky, L., & Ben-Shabat, S. (2015). Effect of medicinal plants on wound healing. *Wound Repair and Regeneration*, *23*, 171–183. https://doi.org/10.1111/wrr.12274

Cesur, S. (2022). Production of gentamycin-loaded poly(vinyl alcohol)/gelatin nanofiber by electrospinning method as wound dressing material. *Konya Journal of Engineering Sciences*, *10*(4), 878–888. https://doi.org/10.36306/konjes.1124919

Chen, S., Liu, B., Carlson, M. A., Gombart, A. F., Reilly, D. A., & Xie, J. (2017). Recent advances in electrospun nanofibers for wound healing. *Nanomedicine*, *12*(11), 1335. https://doi.org/10.2217/nnm-2017-0017

Conti, B., Giunchedi, P., Genta, I., & Conte, U. (2000). The preparation and in vivo evaluation of the wound-healing properties of chitosan microspheres. *STP Pharma Sciences*, *10*, 101–104.

Demirci, T., Hasköylü, M. E., Eroğlu, M. S., Hemberger, J., & Öner, E. T. (2020). Levan-based hydrogels for controlled release of amphotericin b for dermal local antifungal therapy of candidiasis. *European Journal of Pharmaceutical Sciences*, *145*, 105255. https://doi.org/10.1016/j.ejps.2020.105255

Dhandayuthapani, B., Krishnan, U. M., & Sethuraman, S. (2010). Fabrication and characterization of chitosan-gelatin blend nanofibers for skin tissue engineering. *Journal of Biomedical Materials Research Part B: Applied Biomaterials*, *94*(1), 264–272. https://doi.org/10.1002/jbm.b.31651

Dorai, A. A. (2012). Wound care with traditional, complementary, and alternative medicine. *Indian Journal of Plastic Surgery*, *45*, 418–424. https://doi.org/10.4103/0970-0358.101331

Ehrhardt, C., Hrincius, E. R., Korte, V., Mazur, I., Droebner, K., Poetter, A., Dreschers, S., Schmolke, M., Planz, O., & Ludwig, S. (2007). A polyphenol-rich plant extract, CYSTUS052, exerts anti-influenza virus activity in cell culture without toxic side effects or the tendency to induce viral resistance. *Antiviral Research*, *76*, 38–47. https://doi.org/10.1016/j.antiviral.2007.05.002

Erdoğmuş, S. F., Altıntaş, Ö. E., & Çelik, S. (2023). Production of fungal chitosan and fabrication of fungal chitosan/polycaprolactone electrospun nanofibers for tissue engineering. *Microscopy Research and Technique*, *86*, 1309–1321. https://doi.org/10.1002/jemt.24315

Eroglu, Ö. E., Özbek Çelik, B., & Mat, A. (2019). Antimicrobial activities of five endemic hypericum species from Anatolia compared with *Hypericum perforatum*. *Journal of Research in Pharmacy*, *23*(1), 114–119. https://doi.org/10.12991/jrp.2018.115

Fathi, A., Khanmohammadi, M., Goodarzi, A., Foroutani, L., Mobarakeh, Z. T., Saremi, J., Arabpour, Z., & Ai, J. (2020). Fabrication of chitosan-polyvinyl alcohol and silk electrospun fiber seeded with differentiated keratinocyte for skin tissue regeneration in an animal wound model. *Journal of Biological Engineering*, *14*(27), 1–14. https://doi.org/10.1186/s13036-020-00249-y

Gonzalez, A. C. O., Costa, T. F., Andrade, Z. A., & Medrado, A. E. A. P. (2016). Wound healing-a literature review. *Anais Brasileiros de Dermatologia*, *91*(5), 614–620. https://doi.org/10.1590/abd1806-4841.20164741

Hajialyani, M., Tewari, D., Sobarzo-Sanchez, E., Nabavi, S. M., Farzaei, M. H., & Abdollahi, M. (2018). Natural product-based nanomedicines for wound healing purposes: Therapeutic targets and drug delivery systems. *International Journal of Nanomedicine*, *13*, 5023–5043. https://doi.org/10.2147/IJN.S174072

Hashemi, S. S., Saadatjo, Z., Mahmoudi, R., Delaviz, H., Bardania, H., Rajabib, S. S., Mohammad, R. F., Mehrzad, M. Z., & Barmak, J. (2022). Preparation and evaluation of polycaprolactone/chitosan/Jaft biocompatible nanofibers as a burn wound dressing. *Burns*, *48*(7), 1690–1705. https://doi.org/10.1016/j.burns.2021.12.009

Huang, Z. M., Zhang, Y. Z., Kotaki, M., & Ramakrishna, S. (2003). A review of polymer nanofibers by electrospinning and their applications in nanocomposites. *Composites Science and Technology*, *63*(15), 2223–2253. https://doi.org/10.1016/S0266-3538(03)00178-7

Khodja, A. N., Mahlous, M., Tahtat, D., Benamer, S., Youcef, S. L., Chader, H., Mouhoub, L., Sedgelmaci, M., Ammi, N., Mansouri, M. B., & Mameri, S. (2013). Evaluation of healing activity of PVA/chitosan hydrogels on deep second degree burn: Pharmacological and toxicological tests. *Burns*, *39*(1), 98–104. https://doi.org/10.1016/j.burns.2012.05.021

Khoshraftar, Z., Safekordi, A. A., Shamel, A., & Zaefzadeh, M. (2019). Synthesis of natural nanopesticides with the origin of *Eucalyptus globulus* extract for pest control. *Green Chemistry Letters and Reviews*, *12*, 286–298. https://doi.org/10.1080/17518253.2019.1643930

Khoshraftar, Z., Shamel, A. A., Safekordi, A. A., Ardjmand, M., & Zaefizadeh, M. (2020). Natural nano pesticides with origin of *Plantago major* seeds extract for *Tribolium castaneum* control. *Journal of Nanostructure in Chemistry*, *10*, 255–264. https://doi.org/10.1007/s40097-020-00346-w

Küpeli, E., Orhan, D. D., & Yeşilada, E. (2006). Effect of *Cistus laurifolius* L. leaf extracts and flavonoids on acetaminophen-induced hepatotoxicity in mice. *Journal of Ethnopharmacology*, *103*, 455–460. https://doi.org/10.1016/j.jep.2005.08.038

Latiff, N. A., Ong, P. Y., Abd Rashid, S. N. A., Abdullah, L. C., Mohd Amin, N. A., & Fauzi, N. A. M. (2021). Enhancing recovery of bioactive compounds from *Cosmos caudatus* leaves via ultrasonic extraction. *Scientific Reports*, *11*, 17297. https://doi.org/10.1038/s41598-021-96623-x

Levengood, S. L., Erickson, A. E., Chang, F., & Zhang, M. (2017). Chitosan-poly(caprolactone) nanofibers for skin repair. *Journal of Materials Chemistry B*, *5*(9), 1822–1833. https://doi.org/10.1039/C6TB03223K

Matei, A. M., Caruntu, C., Tampa, M., Georgescu, S. R., Matei, C., Constantin, M. M., Constantin, T. V., Calina, D., Ciubotaru, D. A., Badarau, I. A., Scheau, C., & Caruntu, A. (2021). Applications of nanosized-lipid-based drug delivery systems in wound care. *Applied Sciences*, *11*(11), 4915. https://doi.org/10.3390/app11114915

Maver, T., Maver, U., Stana Kleinschek, K., Smrke, D. M., & Kreft, S. (2015). A review of herbal medicines in wound healing. *International Journal of Dermatology*, *54*, 740–751. https://doi.org/10.1111/ijd.12766

Müller, R. H., & Keck, C. M. (2004). Challenges and solutions for the delivery of biotech drugs- a review of drug nanocrystal technology and lipid nanoparticles. *Journal of Biotechnology*, *113*, 151–170. https://doi.org/10.1016/j.jbiotec.2004.06.007

Pachuau, L. (2015). Recent developments in novel drug delivery systems for wound healing. *Expert Opinion on Drug Delivery*, *2*(12), 1895–1909. https://doi.org/10.1517/17425247.2015.1070143

Palamthodi, S., & Lele, S. S. (2014). Nutraceutical applications of gourd family vegetables: *Benincasa hispida*, *Lagenaria siceraria*, and *Momordica charantia*. *Biomedicine & Preventive Nutrition*, *4*, 15–21. https://doi.org/10.1016/j.bionut.2013.03.004

Pereira, R. F., & Bartolo, P. J. (2016). Traditional therapies for skin wound healing. *Advances in Wound Care*, *5*, 208–229. https://doi.org/10.1155/2017/4214382

Poudel, A., Gachumi, G., Wasan, K. M., Bashi, Z. D., El-Aneed, A., & Badea, I. (2009). Development and characterization of liposomal formulations containing phytosterols extracted from canola oil deodorizer distillate along with tocopherols as food additives. *Pharmaceutics*, *11*(4), 185–200. https://doi.org/10.3390/pharmaceutics11040185

Ramakrishna, S., Fujihara, K., Teo, W. E., Lim, T. C., & Ma, Z. (2005). An introduction to electrospinning and nanofibers. *Electrospin Nanofiber*, 396. https://doi.org/10.1142/5894

Ravichandran, S., Jegathaprathaban, R., Radhakrishnan, J., Usha, R., Vijayan, V., & Teklemariam, A. (2022). An investigation of electrospun

Clerodendrum phlomidis leaves extracts infused polycaprolactone nanofiber for in vitro biological application. *Bioinorganic Chemistry and Applications*, *2022*, 1–16. https://doi.org/10.1155/2022/2335443

Rodrigues, M., Kosaric, N., Clark, A. B., & Gurtner, G. C. (2019). Wound healing: A cellular perspective. *Physiology Review*, *99*, 665–706. https://doi.org/10.1152/physrev.00067.20176650031-9333/19

Sadhu, S. K., Okuyama, E., Fujimoto, H., Ishibashi, M., & Yeşilada, E. (2006). Prostaglandin inhibitory and antioxidant components of *Cistus laurifolius*, a Turkish medicinal plant. *Journal of Ethnopharmacology*, *108*(3), 371–378. https://doi.org/10.1016/j.jep.2006.05.024

Sayah, K., Chemlal, L., Marmouzi, M., El-Jemli, Y., Cherrah, M., & Faouzi, A. (2017). In vivo anti-inflammatory and analgesic activities of *Cistus salviifolius* (L.) and *Cistus monspeliensis* (L.) aqueous extracts. *South African Journal of Botany*, *113*, 160–163. https://doi.org/10.1016/j.sajb.2017.08.015

Schreml, S., Szeimies, R. M., Prantl, L., Landthaler, M., & Babilas, P. (2010). Wound healing in the 21st century. *Journal of the American Academy of Dermatology*, *63*(5), 866–881. https://doi.org/10.1016/j.jaad.2009.10.048

Sitterberg, J., Özçetin, A., Ehrhardt, C., & Bakowsky, U. (2010). Utilising atomic force miroscopy for the characterization of nanoscale drug delivery systems. *European Journal of Pharmaceutics and Biopharmaceutics*, *74*, 2–13. https://doi.org/10.1016/j.ejpb.2009.09.005

Stepien, A., Aebisher, D., & Bartusik Aebisher, D. (2018). Biological properties of *cistus* species. *Eur J Clin Exp Med*, *16*, 127–132. https://doi.org/10.15584/ejcem.2018.2.8

Subbiah, T., Bhat, G. S., Tock, R. W., Parameswaran, S., & Ramkumar, S. S. (2005). Electrospinning of nanofibers. *Journal of Applied Polymer Science*, *96*, 557–569. https://doi.org/10.1002/app.21481

Suntar, I. P., Akkol, E. K., Yilmazer, D., Baykal, T., Kirmizibekmez, H., Alper, M., & Yeşilada, E. (2010). Investigations on the in vivo wound healing potential of *Hypericum perforatum* L. *Journal of Ethnopharmacology*, *127*, 468–477. https://doi.org/10.1016/j.jep.2009.10.011

Uhl, K. V., Furnschlief, E., Wagner, A., Ferko, B., & Katinger, H. (2001). Topically applied liposome encapsulated superoxide dismutase reduces postburn wound size and edema formation. *European Journal of Pharmaceutical Sciences*, *14*, 63–67. https://doi.org/10.1016/S0928-0987(01)00149-X

Vargas, E. A. T., Vale Baracho, N. C., Brito, J., & Queiroz, A. A. A. (2010). Hyperbranched polyglycerol electrospun nanofibers for wound dressing applications. *Acta Biomaterialia*, *6*(3), 1069–1078. https://doi.org/10.1016/j.actbio.2009.09.018

Walker, H. L., & Mason, A. D. (1968). A standard animal burn. *Journal of Trauma*, *8*, 1049–1051. https://doi.org/10.1097/00005373-196811000-00006

SUPPORTING INFORMATION

Additional supporting information can be found online in the Supporting Information section at the end of this article.

How to cite this article: Erdoğmuş, S. F., Altintaş, Ö. E., Demirel, H. H., & Okumuş, N. (2023). Fabrication of wound dressings: Herbal extract-loaded nanoliposomes embedded in fungal chitosan/polycaprolactone electrospun nanofibers for tissue regeneration. *Microscopy Research and Technique*, 1–13. https://doi.org/10.1002/jemt.24438